Supporting Material

Supramolecular non-amyloid intermediates in the early stages of α-synuclein aggregation

Jonathan A. Fauerbach[†], *Dmytro A. Yushchenko*[‡], *Sarah H. Shahmoradian*[§¶], *Wah Chiu*[§¶], *Thomas M. Jovin*[‡*], *Elizabeth A. Jares-Erijman*[†*]

[†]Departamento de Química Orgánica, Facultad de Ciencias Exactas y Naturales, Universidad de Buenos Aires (UBA), CIHIDECAR CONICET, Buenos Aires, Argentina, [‡]Laboratory of Cellular Dynamics, Max Planck Institute for Biophysical Chemistry (MPIbpc), Göttingen, Germany and Laboratorio Max Planck de Dinámica Celular (UBA), [§]Department of Molecular Physiology and Biophysics, [¶]National Center for Macromolecular Imaging, and the Verna and Marrs McLean Department of Biochemistry and Molecular Biology, Baylor College of Medicine, Houston, TX 77030, USA.

*__Corresponding authors__: Prof. Dr. Elizabeth A. Jares-Erijman, Departamento de Química Orgánica, Facultad de Ciencias Exactas y Naturales, Universidad de Buenos Aires (UBA), Ciudad Universitaria, Intendente Güiraldes 2160, 1428 Buenos Aires, Argentina. Tel/Fax: +54-11-4576-3346; e-mail: eli@qo.fcen.uba.ar; Dr. Thomas M. Jovin, Max Planck Institute for Biophysical Chemistry, am Fassberg 11, 37077 Göttingen, Germany. Tel: +49-551-2011382; Fax: +49-551-2011467; Email: tjovin@gwdg.de.

Purification, labeling and preparation of α-synuclein

AS purification. Wildtype human α-synuclein (wtAS) and monocysteine mutants were expressed in *E. coli* BL21 (DE3) cells. The production of the recombinant protein was according to a 2009-2010 protocol (currently being revised) of the Laboratory of Cellular Dynamics (MPIbpc). Transformation was with pT7-7 plasmids encoding wildtype and mutant protein sequences. Expression was initiated by inoculation of a volume of 900 ml LB medium with 100 ml of a pre-culture and addition of 1 ml of 100 mg/ml ampicilin. Incubation was carried out at 37 °C with agitation (400 rpm) until the A_{600} reached a value of 0.5-0.8. Expression of the recombinant protein was induced by addition of IPTG and incubation was continued for an additional 4-6 h. The bacterial cells were harvested by centrifugation (Beckman JA10 rotor, 5000 rpm, 30 min 4 °C) and the pellets were stored at -20 °C. Cell pellets were thawed with 15- 20 ml lysis buffer containing 10 mM Tris-HCl, pH 7.7, 1 mM EDTA and 1 mM protease inhibitor PMSF. In the case of cysteine-containing mutants, 5 mM dithiothreitol (DTT) was added. Three freeze-thaw cycles were performed with liquid N_2 and 70 °C hot water. The cells were lysed by sonication using a Fisher Scientific Digital Sonic Dismembrator Model 500 with a 6.5 mm diameter Branson microtip. Cells were subjected to three 10 s periods of sonication at 50% maximum amplitude, with 10 s intervals on ice. The extract was centrifuged 15 min at 2500×*g* and the supernatant was recovered. Proteins other than AS were denatured/precipitated by boiling at 100 °C for 20 min followed by centrifugation at 37000×*g* for 30 min at 4 °C. DNA was removed by addition of streptomycin sulfate to the supernatant to a final concentration of 10 mg/ml, agitation of the solution for 15 min at 4 °C, and centrifugation for 30 min at 4 °C and 37000×*g*. AS was precipitated from the supernatant by addition of solid $(NH_4)_2SO_4$ to a final concentration of 360 mg/ml and subsequent centrifugation as above. The pellets containing AS were stored at -20 °C. Purification of AS was carried out with a GE Healthcare ÄKTA explorer FPLC system equipped

with an Applied Biosystems POROS HQ 20 µm, 4.6×100 mm (1.7 ml) column. Samples were concentrated with Millipore Amicon 10 kDa filters and ultracentrifuged for 1 hour at $10^5 \times g$ in a Beckman 80 TLS-55 rotor. The supernatant was recovered, diluted to a convenient concentration and frozen with liquid N_2, with storage at -80 ºC.

Protein labeling. MFC was synthesized as described (1). For the labeling procedure, MFC was dissolved in DMSO and mixed dropwise with a solution of ~300 µM AS-A140C in 25 mM Na-PO_4 pH 7.3, 3 mM tris(2-carboxyethyl)phosphine (TCEP) ; the final DMSO:buffer ratio was 1:2. MFC was in a 5-10-fold molar excess over the protein. After the complete addition of the MFC-DMSO solution and confirming the lack of a precipitate, the mixture was left at 4 ºC under stirring overnight (ON). The next day the reaction mixture was diluted 10-fold with 25 mM Na-PO_4 pH 7.3, 3 mM TCEP and concentrated by 3-4 passages through a Millipore Amicon 10 kDa filter to a volume of ~ 1 ml in order to remove DMSO from the reaction mixture. A size exclusion PD-10 column was used as a first step of purification from the unbound dye. A Pharmacia Smart chromatography system was used with a Superdex 200 column (10/300) and 25 mM Tris-HCl, pH 7.2, 150 mM NaCl elution buffer to separate thoroughly the excess reagent from the labeled protein and the unlabeled protein. The extent of labeling was 50-70%. Samples were frozen with liquid N_2 and stored at -80 ºC.

Aggregation assays. Aggregation assays of wtAS protein incubated together with labeled AS with the MFC ESIPT probe were performed at 37 and 70 ˚C in 5×5 mm Hellma 111.057-QS cuvettes, tightly sealed with Teflon stoppers to avoid solvent evaporation. Mixing was done with a parylene coated tumble disk (V&P Scientific, San Diego CA). Aggregation assays were performed in a continuous manner in a temperature controlled Cary Eclipse spectrofluorometer (Varian, Australia) (1). The excitation wavelength was 345 nm with a 342±10 nm bandpass filter added to suppress scattering of out-of-band light. The excitation and emission slits were adjusted to 5 mm. Fluorescence spectra were recorded from 365-700 nm every 30 min during the first 48 h of reaction and every 1 h thereafter up to 180 h. The ESIPT N* and T* bands were located at 420 and 520 nm, respectively. Mixers were fixed at 600 rpm and controlled by a homemade stirring device controlled by a National Instruments LabVIEW VI script generated in the Laboratory of Cellular Dynamics. The aggregation buffer was 25 mM Na-PO_4, pH 6.2, 0.02% NaN_3. ThioT assays were performed in 50 mM Na-glycine buffer, pH 8.2, with excitation at 446 nm and emission at 482 nm. Two types of samples were prepared for *in vitro* aggregation experiments: a) 97.5% wtAS + 2.5% AS140-MFC, and b) 100% wtAS. The total protein concentration was 150 µM in all cases. In the case of cold agregations, the temperature was maintained at 4˚C without agitation. Samples were taken at given intervals for AFM measurements.

Ultracentrifugation of AS monomer. In order to achieve reproducible conditions and results in the aggregation assays, it is important to clear the starting material of sub-µm aggregates. Ultracentrifugation (1 h at $10^5 \times g$) was effective. Fig. S1 shows a sample of monomeric wtAS before and after ultracentrifugation; the importance of this step is apparent.

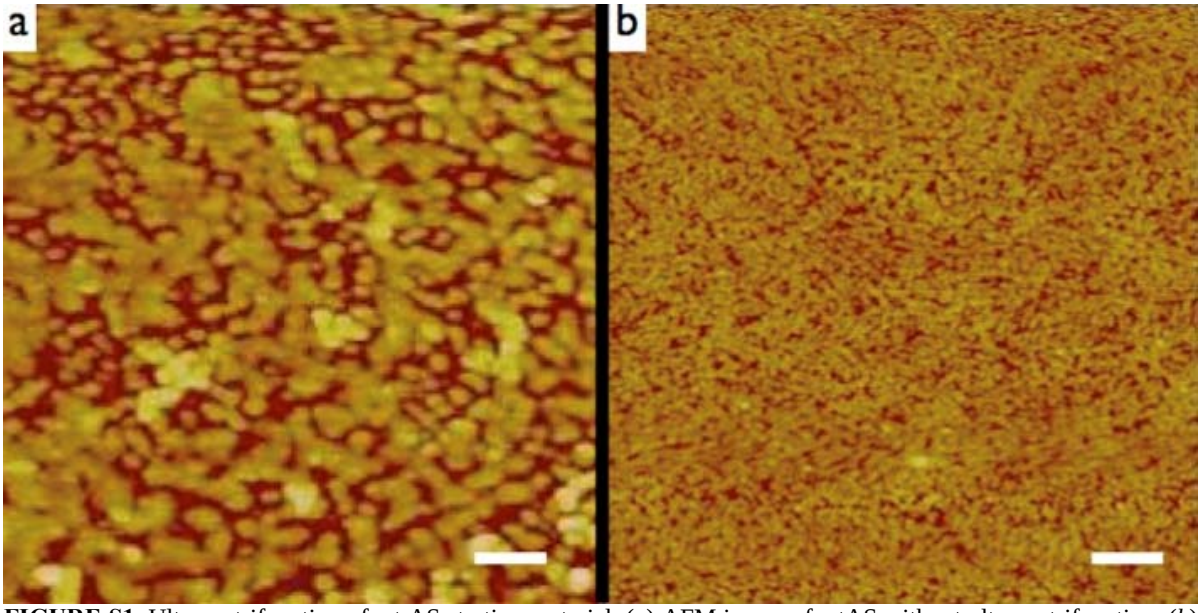

FIGURE S1. Ultracentrifugation of wt AS starting material. (*a*) AFM image of wtAS without ultracentrifugation. (*b*) AFM image of the same sample ultracentrifuged 1 h at $10^5 \times g$. Scale bar, 300 nm.

Atomic force microscopy

Sample preparation. AFM was performed with a Veeco Nanoscope Models III and V, using silicon nitride tips (µmash) with 10 nm radius and 300 KHz drive frequency for air tapping mode imaging. Unless otherwise indicated, samples were applied to freshly cleaved mica surface by spin-coating, a procedure which is very effective in uniformly depositing heterogeneous samples without a directional drying bias by virtue of the very rapid, isotropic loss of solvent normal to the surface. The spin-coating process can be described by 3 stages: a) deposition, b) centrifugation, and c) drying of the sample. In the first stage, 10 µl of a 10-fold dilution of the original sample with Milli-Q water is applied over the mica and left for 1 min to promote interactions with the substrate. The substrate is then accelerated up to the final desired rotation speed (typically 2000 rpm), leading to aggressive fluid expulsion from the surface due to the centrifugal force. The final stage consists of the substrate spinning at a constant rate for a given time (generally 2 min), during which solvent evaporation dominates the processes of thinning and coating. The samples are then ready for AFM imaging, and can be maintained for >1 year at room temperature without signs of significant degradation in subsequent scans (see Figs. S13, 14).

AFM controls. After thorough study of the *in vitro* aggregation of wtAS using 3% of labeled protein with the MFC probe, we decided to use a different probe (pyrene) in order to rule out any direct probe-effects. A 300 µl sample was prepared containing 96% wtAS + 4% AS-A140C-pyrene (2) (total protein concentration 150 µM) in 25 mM Na-PO_4 buffer, pH 6.2. The solution was incubated in a 1.5 ml tube in an Eppendorf thermomixer at 37 ˚C and 600 rpm for 11 h. Figure S2 shows AFM images of a 10-fold dilution of the sample; 10 µl of the dilution was placed over mica and spin-coated.

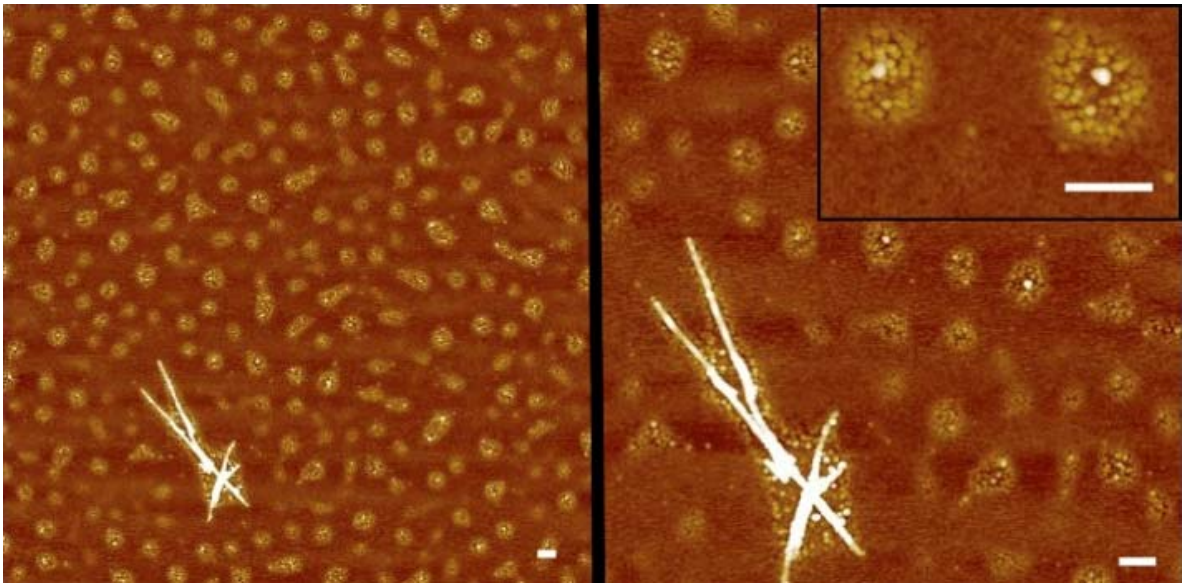

FIGURE S2. AFM images of acunas prepared at 37 ˚C from 96% wtAS + 4% AS-A140C-pyrene in 25 mM Na-PO_4 buffer, pH 6.2, incubated in a thermomixer at 600 rpm for 11 h. A sample was diluted 10-fold with Milli-Q water (final [AS] 14 µM, [buffer] 2.5 mM), applied to freshly cleaved mica and spin-coated.

After confirmation of the presence of acunas, the solution was maintained at 4˚C for 1 week, at which time a new 10-fold dilution was prepared and scanned (Fig. S3). Acunas were still present, indicating that cooling to 4 ˚C had aborted the aggregation reaction and preserved the acuna intermediates.

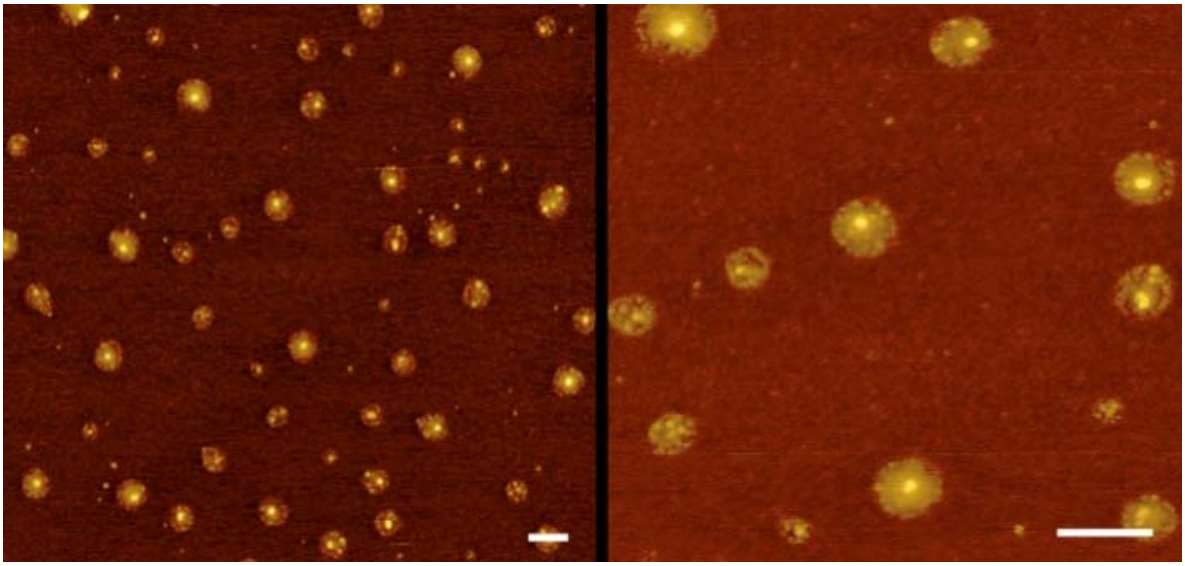

FIGURE S3. AFM images of the sample shown in Fig S2 and kept at 4 ˚C for 1 week. The sample was diluted 10-fold with Milli-Q water and spin-coated over mica. Scale bar, 300 nm.

Five µl of the same dilution (preserved in ice for 2 h) was placed on a new mica disk and allowed to evaporate during 30 min. inside a Petri dish. After the drop disappeared, the substrate was exposed to a gentle N_2 stream and then scanned (Fig. S4). Acunas were clearly visible, indicating that they had not arisen as an artifact of the spin-coating procedure.

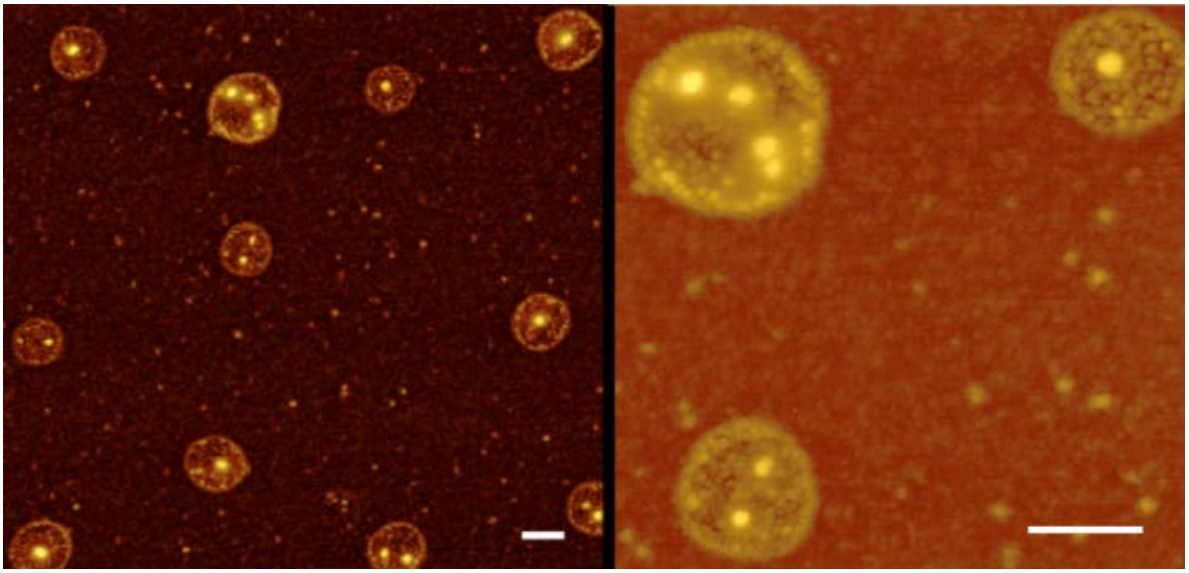

FIGURE S4. AFM images of the sample showed in Fig. S2 but evaporated over mica without spin-coating. [AS] 14 µM and [buffer] 2.5mM. Scale bar, 300 nm.

To study the effects of both salt and protein concentration on the morphology and stability of acunas, the sample described above was diluted a further 2-fold with water and applied to mica without spin-coating (Fig. S5). There was a partial loss in the structural definition of acunas and an increase in the amount of loose material in the background, indicating that the acunas require a certain ionic strength for stability.

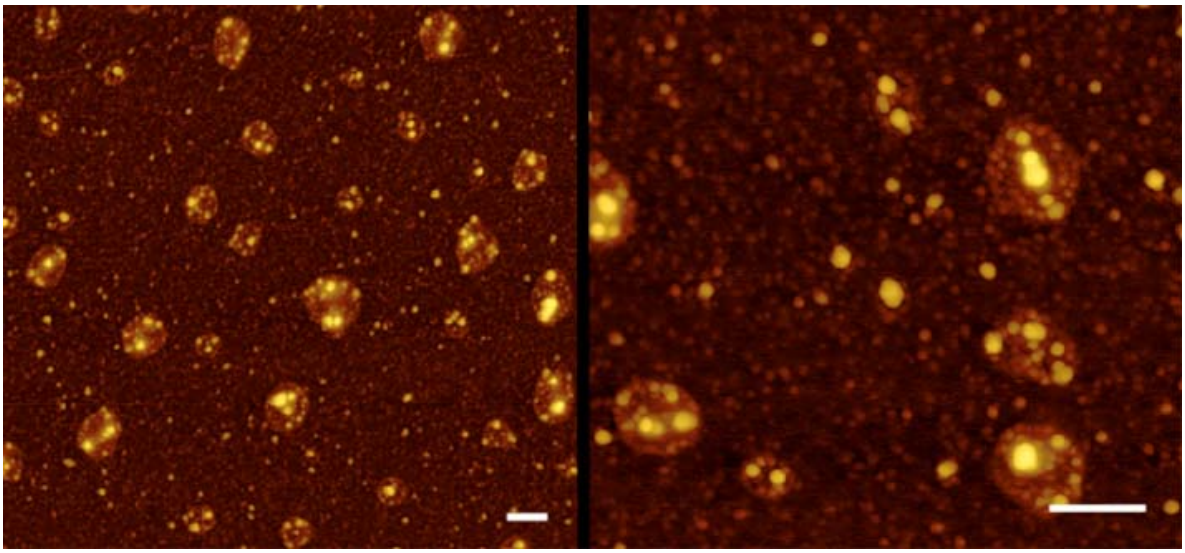

FIGURE S5. AFM images of same sample as in Fig. S2 but diluted an extra 2-fold with water, resulting in a 7 µM final AS concentration and 1.25 mM buffer. The sample was not spin-coated. Scale bar, 300 nm.

From the original sample kept at 4 ˚C (Fig. S2, S3) a new 50-fold dilution was prepared with 2.5 mM buffer, such that the final AS concentration was 3 µM in 2.5 mM buffer (Fig. S6). Acunas were still present and retained their shape, although they were somewhat more compact in appearance with much less loose material visible in the background, compared to Figure S5.

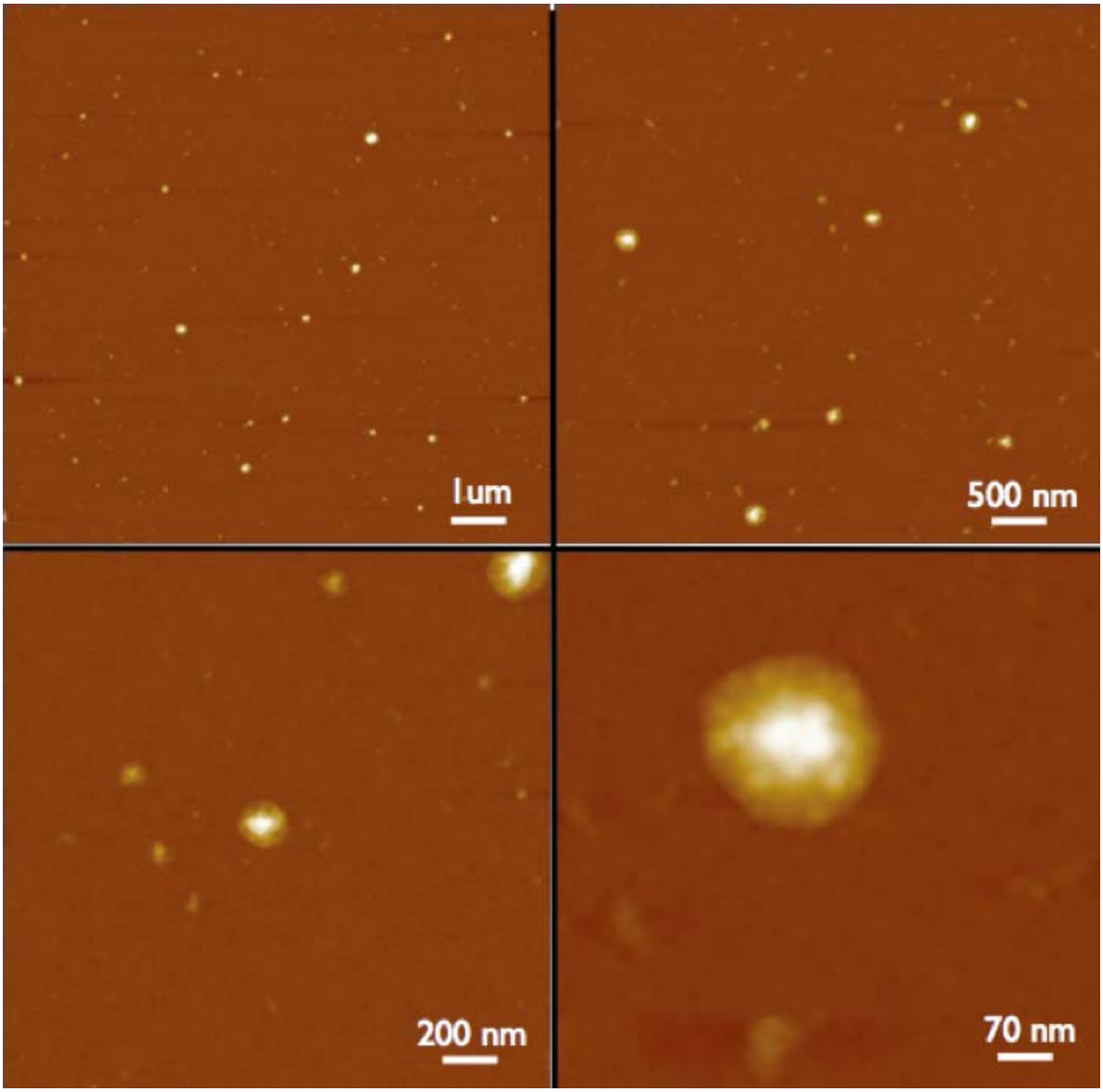

FIGURE S6. AFM images of same sample as in Fig. S2 but diluted an extra 50-fold with water, resulting in a 3 μM final AS concentration and 2.5 mM buffer. The sample was not spin-coated.

Finally, another 50-fold dilution was prepared but this time in 25 mM buffer, yielding 3 μM protein and 25 mM buffer (Fig. S7). Acunas were visible but appeared in groups of 2, 3 or 4 with an intriguing fibrillation and fuzziness apparent on the surface.

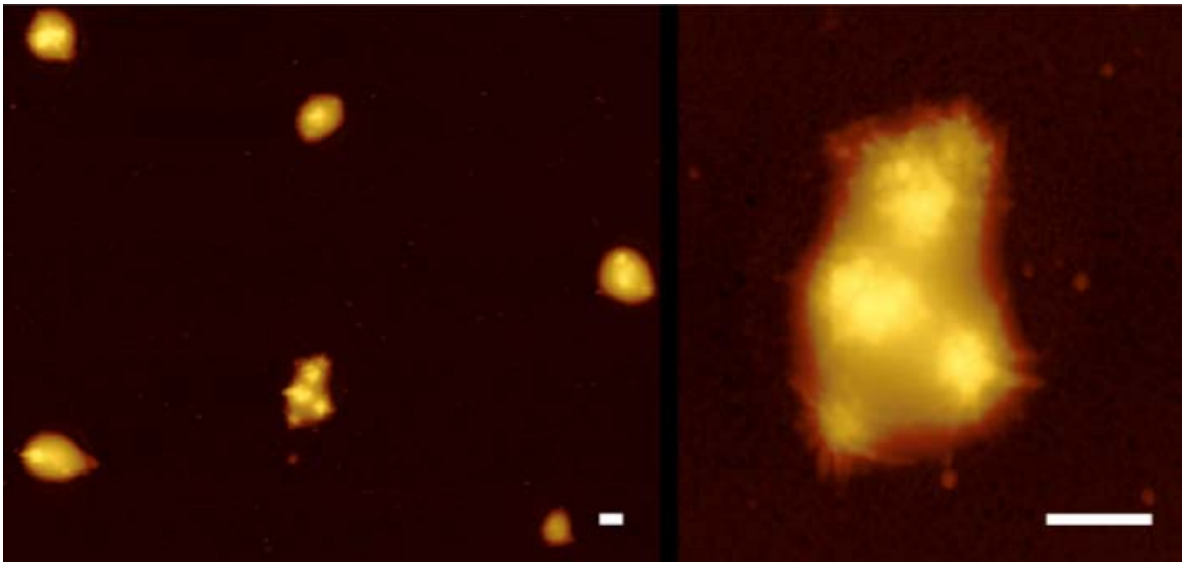

FIGURE S7. AFM image of same sample as in Fig. S2 but further diluted 5-fold with buffer of higher concentration (25 mM), yielding 3 µM protein and 25 mM buffer. Scale bar, 300 nm.

AFM samples are often subjected to washing procedure *in situ* in order to reduce interference from residual salt after drying in air. Figure S8 shows the effect of introducing a washing step in the sample preparation protocol. The protocol was as follows: a) application of 10 µl of sample (10 fold water dilution of original reaction) to freshly cleaved mica; b) 5 min incubation to permit protein-substrate interaction; c) removal of excess solution by capillarity using a paper tissue at the edge; d) application of 100 µl of Milli-Q water; e) removal of liquid after 30 min by wicking with paper tissue; f) repetition of steps d and e; and g) drying with a gentle stream of N_2. The washing steps produced a high background of small particulate material, particularly oligomeric-spheroidal and fuzzy balls. Depressions in the underlying layer are apparent, with the size and shapes of acunas imaged previously. In many cases, fuzzy fibers (see below) and residues of the underlying acuna backbone are present in these areas, indicative of a greater resistance of these structures to low ionic strength conditions.

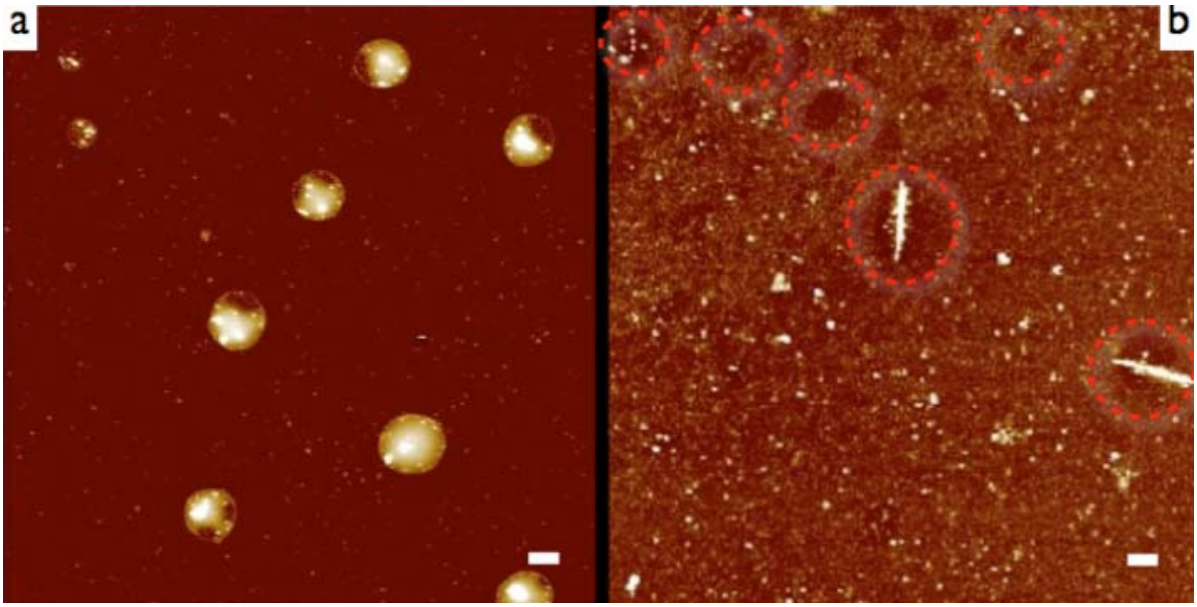

FIGURE S8. Washing out of acunas. (*a*) AFM image of a 10-fold dilution of wtAS + 4% AS-A90C-pyrene incubated 11 hs at 37˚C and then maintained at 4 °C. Sample not spin-coated but dried by evaporation during 30 min. (*b*) same sample treated according to the washing protocol (see above). Scale bar, 500 nm.

Acunas prepared at 4 ˚C were also imaged by AFM under liquid with a Nanoscope V glass liquid cell, and V-shape SiN_2 cantilevers of 0.06 N/m spring constant and 10 KHz drive frequency. A scanning buffer (25 mM Na-PO_4 pH 6.2, 2mM $MgCl_2$) was used to flood the cell holding the cantilever and to dilute the sample. Thirty-to-forty µl of the scanning buffer was used to fill the liquid cell before engaging with the substrate. Air was removed and a hanging drop was formed. The laser was re-aligned and left for 20 min to achieve thermal equilibration. The mica substrate was pretreated with 25 mM $MgCl_2$: 20 µl was spin-coated over the mica, which was then washed twice with 50 µl of water and dried. Forty-to-fifty µl of protein solution was mixed with 10-15 µl of scanning buffer, placed over the mica substrate, and left for 10 min for thermal equilibration and substrate interaction prior to scanning. A "water dome" was formed over the substrate. The final step before scanning was to establish contact between the water and the hanging drop, leading to coalescence. AFM under liquid is more difficult than in air due to the longer scan times required, evaporation of the liquid, dispersion of the sample, thermal effects, and laser position fluctuations; all these effects reduce image quality. The images exhibited a quantity of loose material on the reaction mixture and a lack of adhesion of the supramolecular structures to the substrate. The phase channel helped to visualize the acunas due to their higher density structure. Compact round-oval structures, 300-600 nm in size, were observed, clearly distinguishable from the background, in which loose material was apparent (Fig. S9).

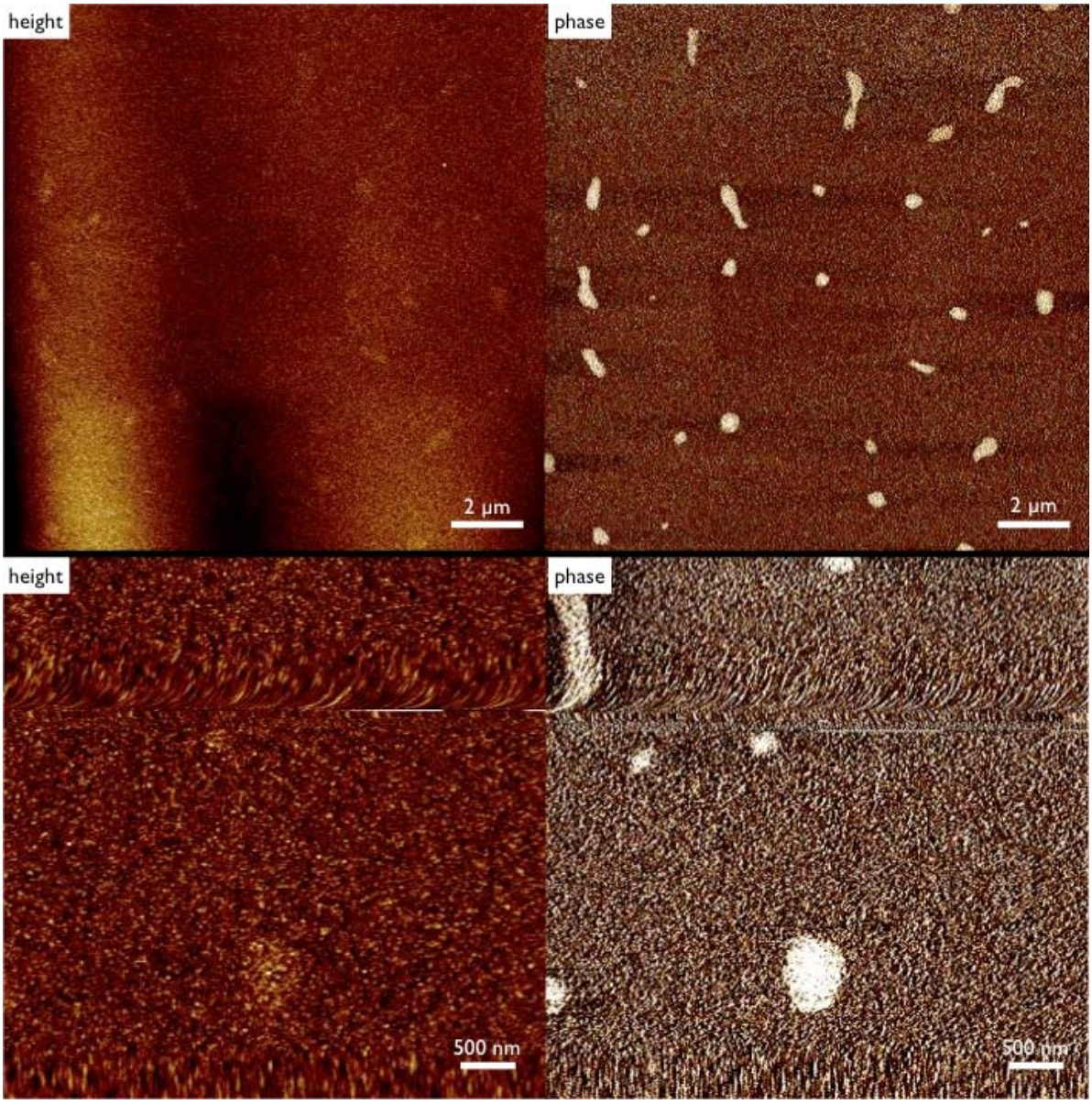

FIGURE S9. AFM images of latent acunas using liquid cell (under-liquid AFM). The height and phase channels are shown individually.

To exclude a potential influence of the mica substrate on sample appearance or orientation, AFM measurements were performed with samples spin-coated on flat glass substrates (Coherent FS superpolish substrate, Catalog# 45-1922-000). The AFM images revealed acunas as well as smaller structures (Fig. S10).

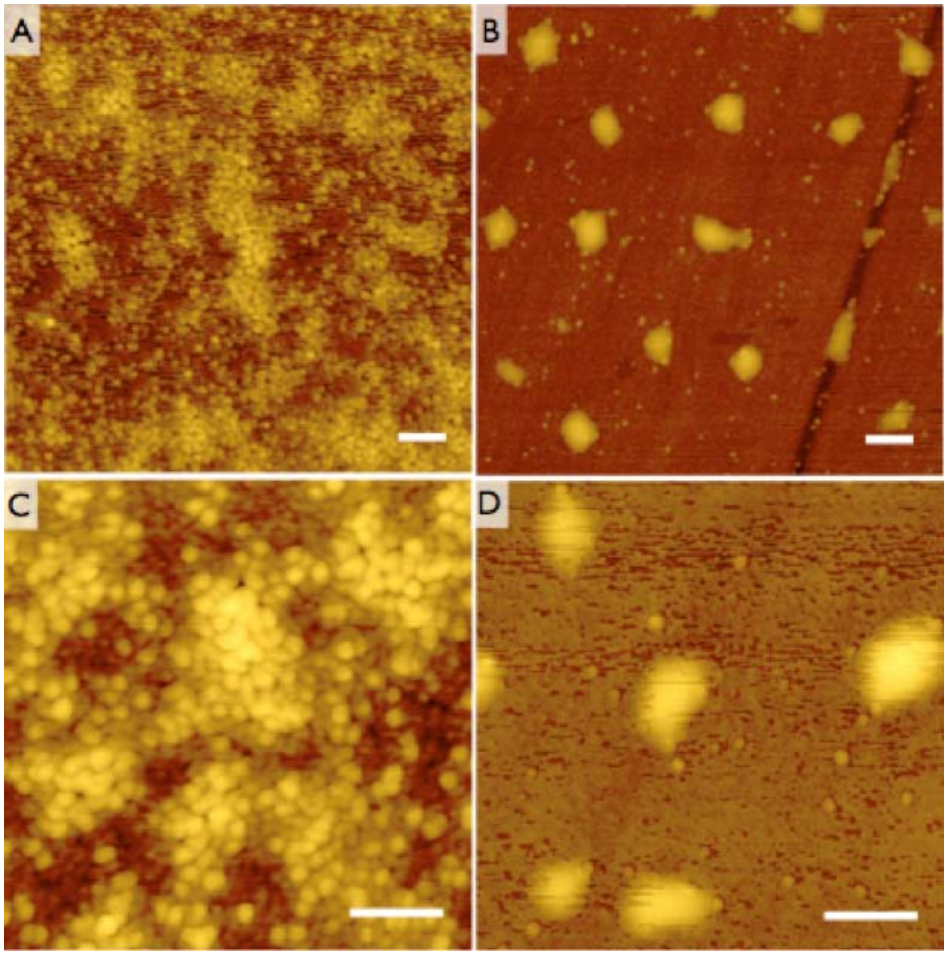

FIGURE S10. AFM images of acunas on a glass surface. A sample of latent acunas prepared at 4 ˚C from 300 µM wtAS was spin-coated on glass discs. (*A, C*) Fields of 10 and 5 µm, respectively, of the sample diluted 10 times with water. (*B, D*) The same sample diluted 20-fold prior deposition on the substrate. Fields of 10 and 5 µm are shown for comparison. Scale bars, 500 nm.

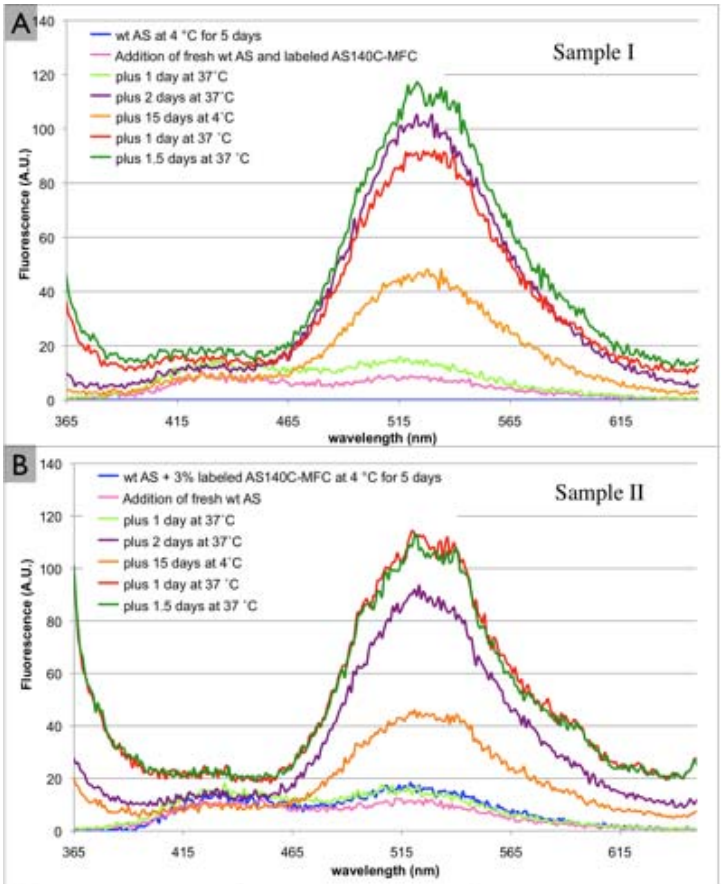

C

			Sample I (AS wt)			Sample II (AS wt + 3% AS*)		
Day	Curve Color	°C	I^{430nm}	I^{525nm}	T*/N*	I^{430nm}	I^{525nm}	T*/N*
5	blue	4	-	-	-	14	15	1.1
2nd Addition of AS	-	-	+ AS wt + 3%AS*			+ AS wt		
	pink	4	9	8.7	0.9	7	10	1.5
6	light green	37	15	14	1	11	12	1.2
7	purple	37	12	101	8.8	12	88	7.4
22	orange	4	9	47	5.4	6	43	7.6
23	red	37	16	89	5.5	16	112	6.8
25	dark green	37	18	115	6.5	18	105	5.8

FIGURE S11. Aggregation of AS samples differing in initial composition and incubated at various temperatures. Two sample were prepared: Sample I, 200 µl of 300 µM wt AS in Na-PO_4, pH 7.4, 0.02% NaN_3; and Sample II, equal to sample I plus 3% of labeled AS-A140C-MFC (AS*). So sample II was initially fluorescent, and sample I not. Emission spectra and AFM (see Fig. S12) were used to follow the temporal evolution. Both samples were incubated at intermittent temperatures, starting at 4 ˚C for 5 days (blue curves). After incubation, fresh protein was then added: 100 µl of 200 µM wtAS to both samples, and 3% labeled AS* to sample I, such that both samples now had exactly the same composition. Incubation was then resumed at 37 ˚C for ~2 days (day 6 and 7 in table, curves light green and purple). Samples were then kept at 4 ˚C for 15 days (day 22 in table, orange curve). Incubation continued for ~2-3 days at 37 ˚C (day 23-25 in table, curves red and dark green). (*A*, *B*) Emission spectra, corrected by initial unlabeled wtAS spectra and volume dilution upon second addition of protein. (*C*) Table of fluorescence intensities of N* and T* bands (430 and 525 nm, respectively), T*/N* ratios, days of incubation and incubation temperatures. The corresponding AFM images are shown in Fig. S12.

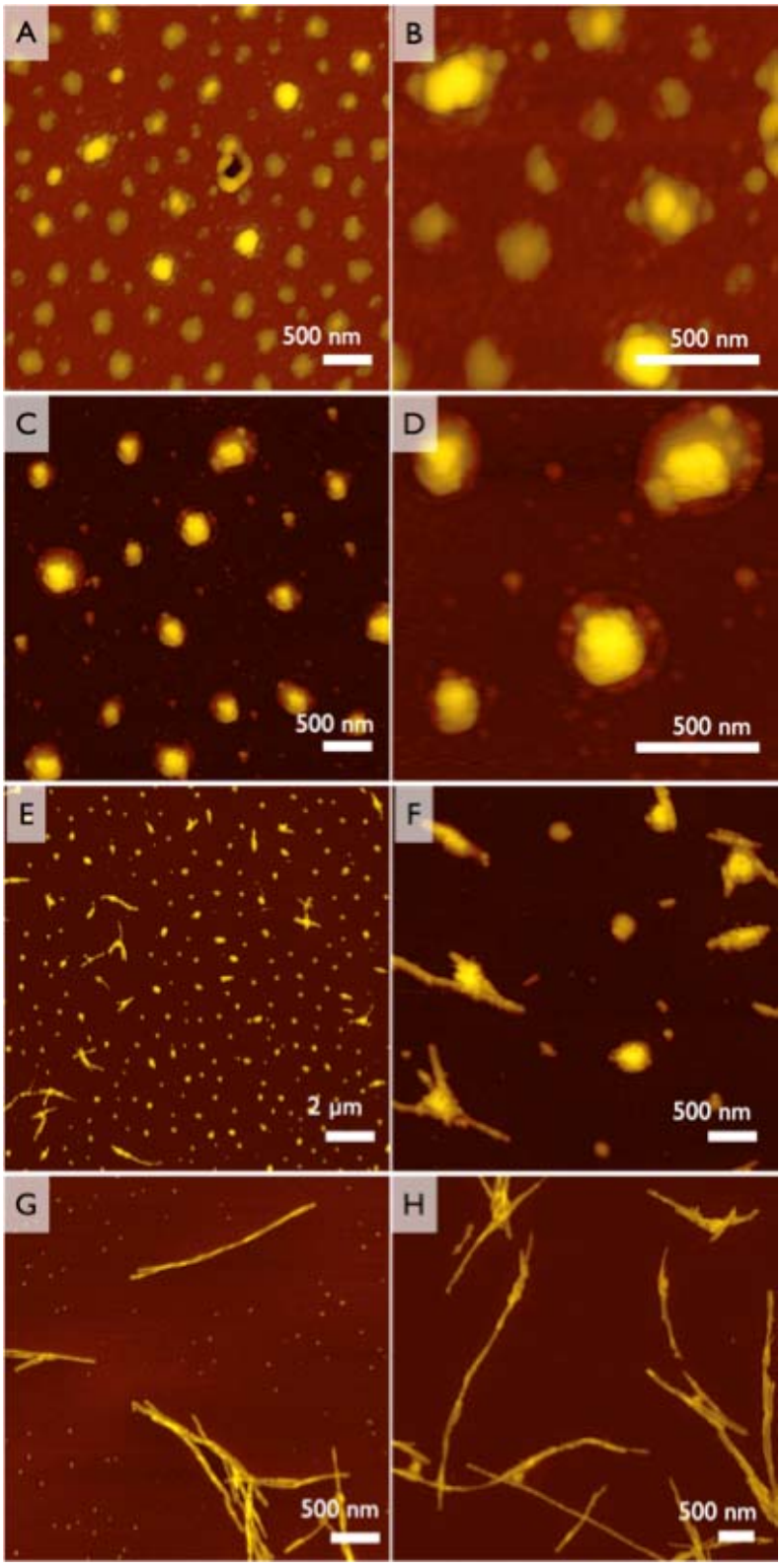

FIGURE S12. AFM images of samples I and II corresponding to Figure S11. (*A, B*) Latent acunas obtained after 5 days of incubation at 4 ˚C of AS (day 5, blue curve). (*C, D*) sample after addition of fresh monomeric AS and incubated 1 day at 37 ˚C (day 6, light green curve). (*E, F*) after incubation for ~2 days at 37 ˚C (day 7, purple curve). (*G*) after incubation during 15 days at 4 ˚C (day 22, orange curve). (*H*) Sample incubated further for ~2-3 days at 37 ˚C (day 25, dark green curve). Panels *A, B, E, F* and *G* correspond to sample I. Panels *C, D* and *H* correspond to sample II. Both samples showed similar, comparable structures.

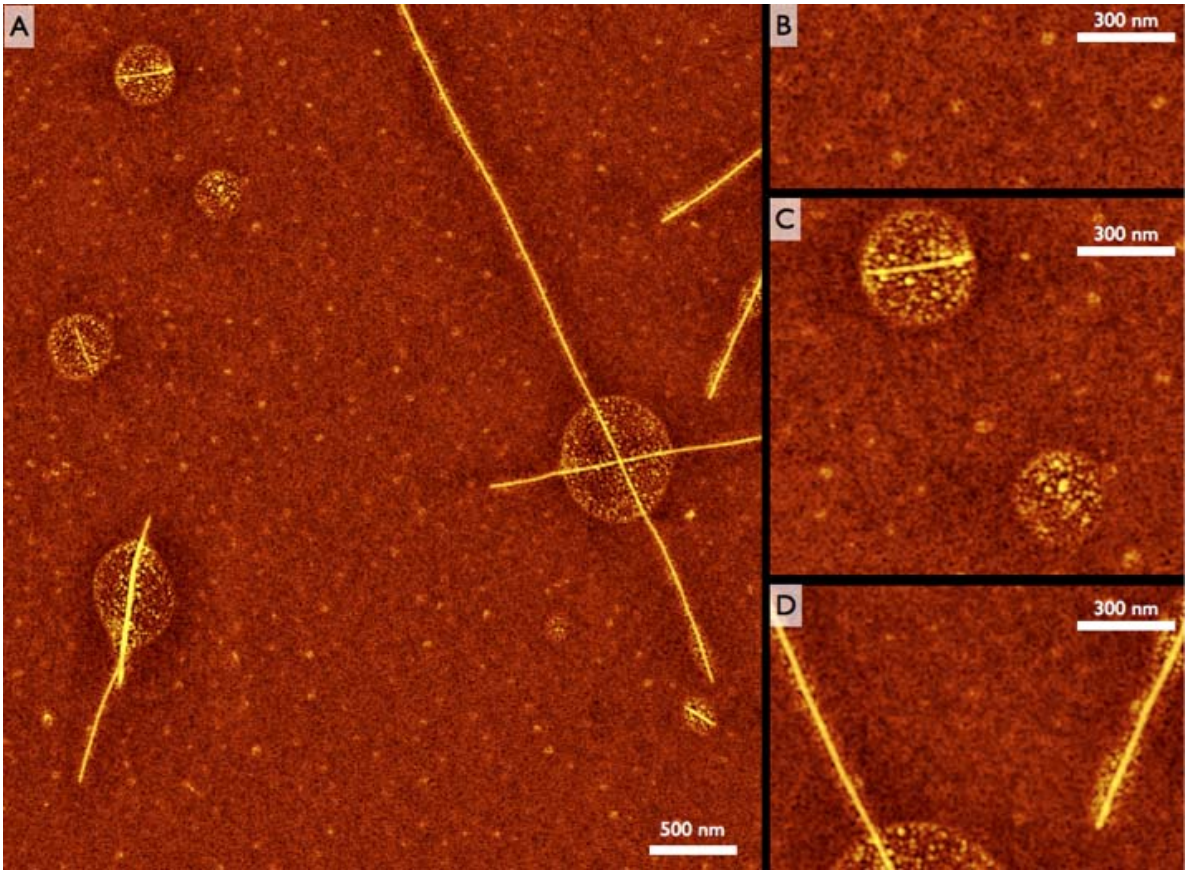

FIGURE S13. (*A*) High resolution AFM image of Fig. 1B (main text) after >1 year of storage. (*B, C, D*) zoom areas of panelA, in which details of the heterogenous species are evident: *fbs*, latent acunas, productive acunas and *ffs*.

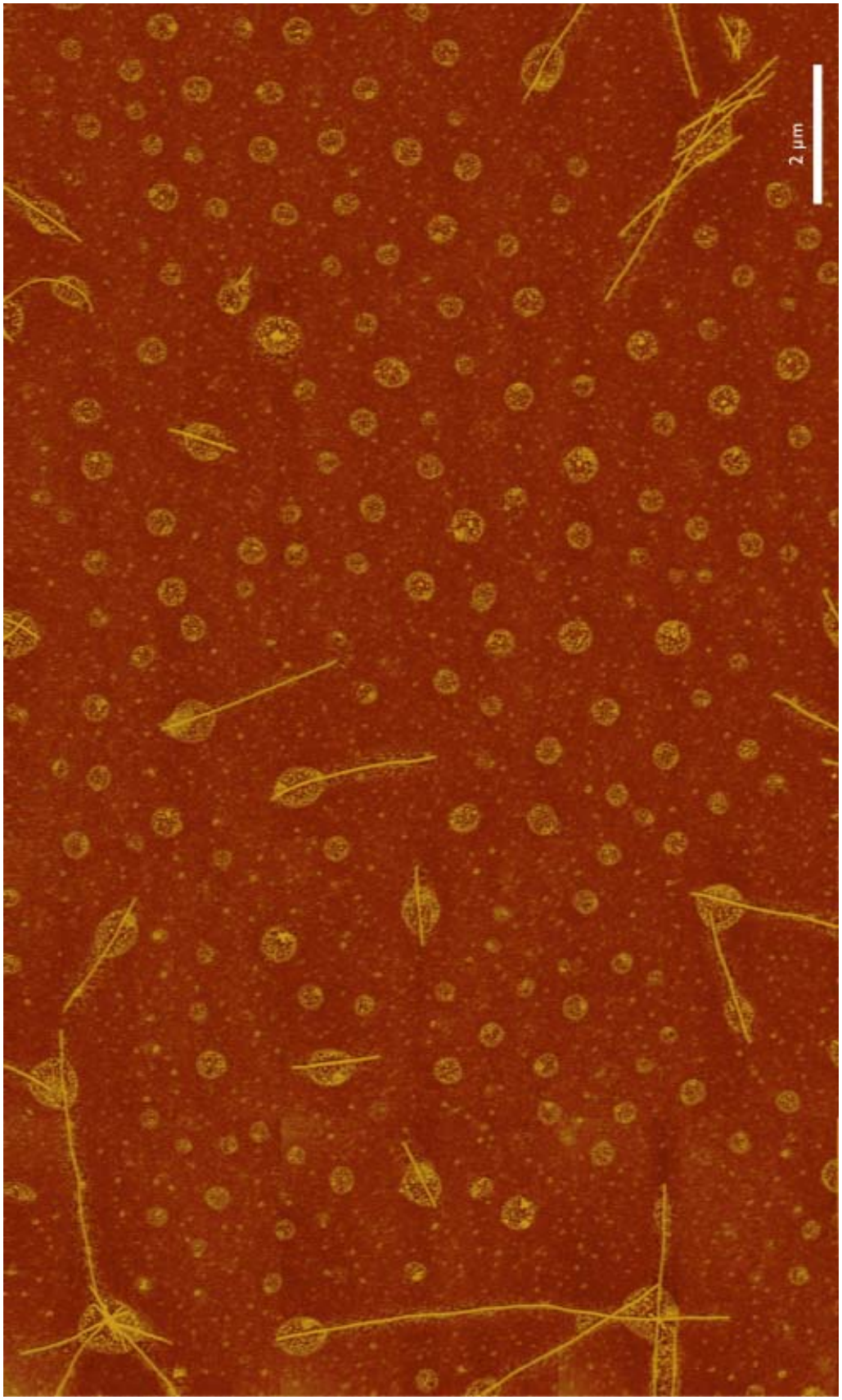

FIGURE S14. High-resolution AFM image of Fig. 1B (main text) after >1 year of storage. Image dimensions, 20×12 µm. The presence of heterogenous species is evident: *fb*s, latent acunas, productive acunas and *ff*s.

AFM morphological analysis. In view of the numerous novel structures observed during the aggregation of AS by AFM sampling, a morphological analysis was carried out in order to define the distinguishing features of the various supramolecular structures. These were subdivided in three main groups: a) balls and fuzzy balls (*fb*s; for definitions of these and other designated entities, see Results), b) latent and productive acunas, and c) fibers and fibrils. Within the last group it was possible to identify at least three different stages of compaction and entanglement. The determinations of topographic height were inherently more reliable than of lateral dimensions in the case of small structures approaching the size of the AFM tip diameter, although in the presence of partial collapse due to drying, and/or masking as a consequence of being embedded in an underlying protein layer to an indeterminate degree, the aparent heights would be underestimates. Images were acquired with Nanoscope IIIA and V and files were opened and flattened with the DIPimage (Quantitative Imaging Group, Delft University of Technology, The Netherlands) MATLAB (The MathWorks, Natick, MA) toolbox using a script of Bernd Rieger and Anthony De Vries based on a published algorithm (3). A batch analysis was performed on multiple images and the resultant images were saved in floating point, preserving the *z*-scale in nm. For the group of *fb*s and acunas we measured the distribution of maximal heights after segmenting the population. Diameters were calculated from the areas using an equivalent circle model, and shape eccentricity from the '*perimeter-to-area'* (P2A) parameter (DIPimage subroutine: '*Size'*, '*SurfaceArea'*).

In the case of fibers and fibrils, the height, diameter, and periodicity were determined using a similar procedure. In these cases selective thresholding (DIPimage subroutine: '*background'* threshold) was used to distinguish the analysis of fibers from *fuzziness*. The diameters of fuzzy fibers (*ff*s) were determined by distance transforms (DIPimage subroutine: *'Size'*, *'Max Val'*, *'SurfaceArea'*), and of the denuded fibers (*df*s) and mature amyloid fibrils (*maf*s) from the combination of the perimeters and areas of equivalent rectangles (DIPimage subroutine: *'Size'*, *'SurfaceArea'*). The periodicity was computed by fitting a sine function to the longitudinal profile through central axis of fibers and fibrils. Statistical analyses were applied to determine means and standard deviations (Table 1).

Cryo-electron tomography

Specimen preparation. Copper grids (Fig. S15a) were rinsed in PBS (Biological Industries) and coated with a thin carbon film as previously described (holey carbon support film (4). The grids were allowed to fully dry before application of 2.5 µL droplet of sample suspension (wtAS + 2.5% AS-A140C-MFC, incubated for 3-4 days at 4 ˚C). After being blotted using Vitrobot Mark III (FEI, Eindhoven), the samples were embedded in vitreous ice by plunging the grids into liquid N_2-cooled ethane, thereby preserving them in a close-to-native conformation without fixation or staining (5). The grids were then transferred to liquid N_2 and inserted into a 200-kV JEM2100 LaB6 cryo-electron microscope (JEOL, Tokyo) with a ±70° tilt cryoholder (Gatan, Pleasanton).

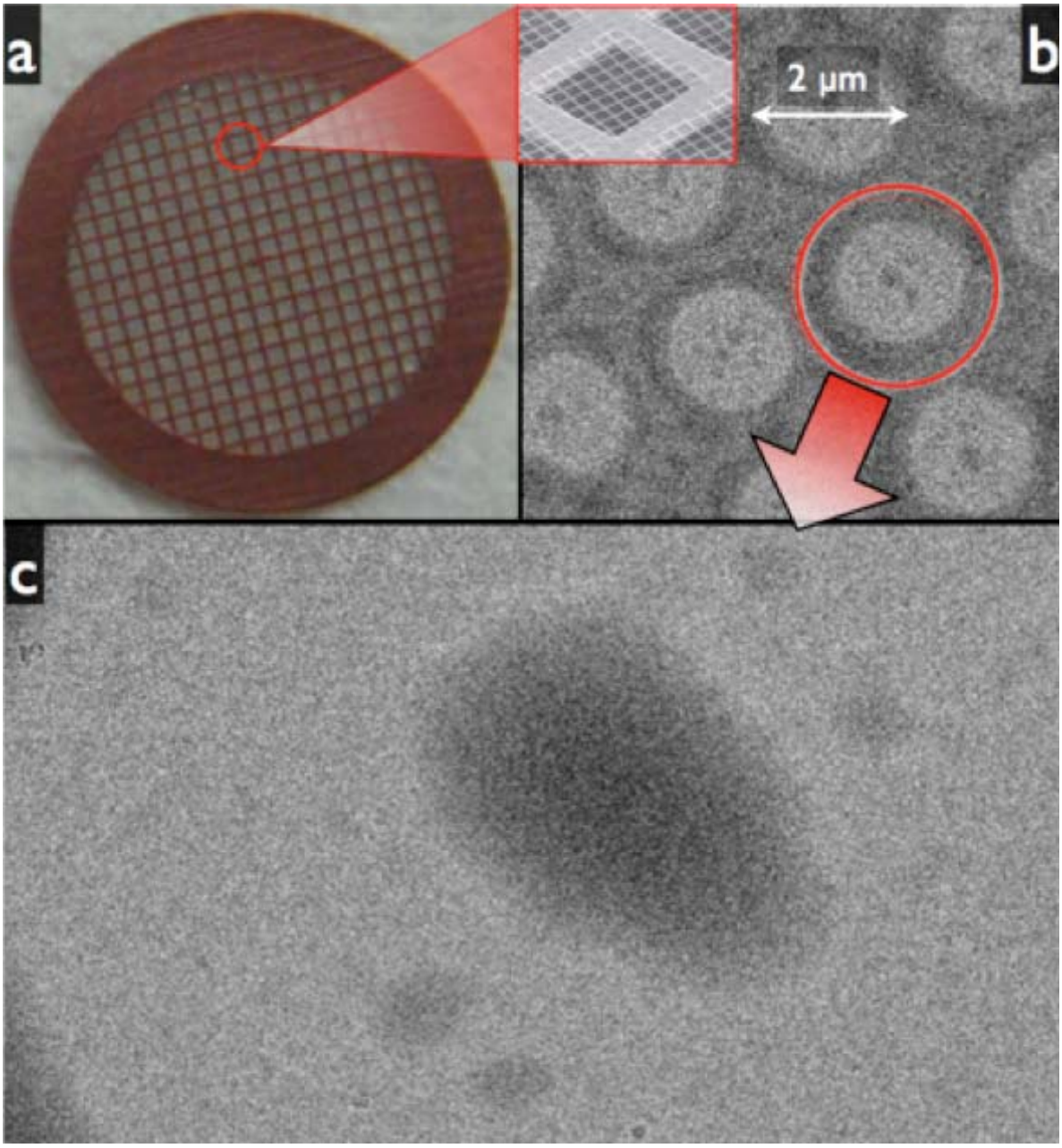

FIGURE S15. Cryo-EM grid and single tomograms of wtAS sample incubated 3-5 days at 4 ˚C (latet acunas). (*a*) Carbon-coated 200-mesh copper grid. (*b*) single cryo-ET tomogram of grid with oblong structures (latent acunas) homogenously deposited over the grid. (*c*) single cryo-ET tomogram of a wtAS acuna (for a complete 3D-tomogram and annotation see Fig. 4).

Electron tomography. Single-axis tilt series were acquired under low-dose conditions with SerialEM tomographic software (6) and targeted at a ~6 µm under-focus. The angular range of the tilt series was -60° to +62°, sampled in 2° tilt increments. Because of the increased specimen thickness at higher tilt angles, the exposure time was varied according to $(\cos \alpha)^{-1}$. The cumulative dose of incident electrons for recording the tilt series was below 70 electrons/Å^2.

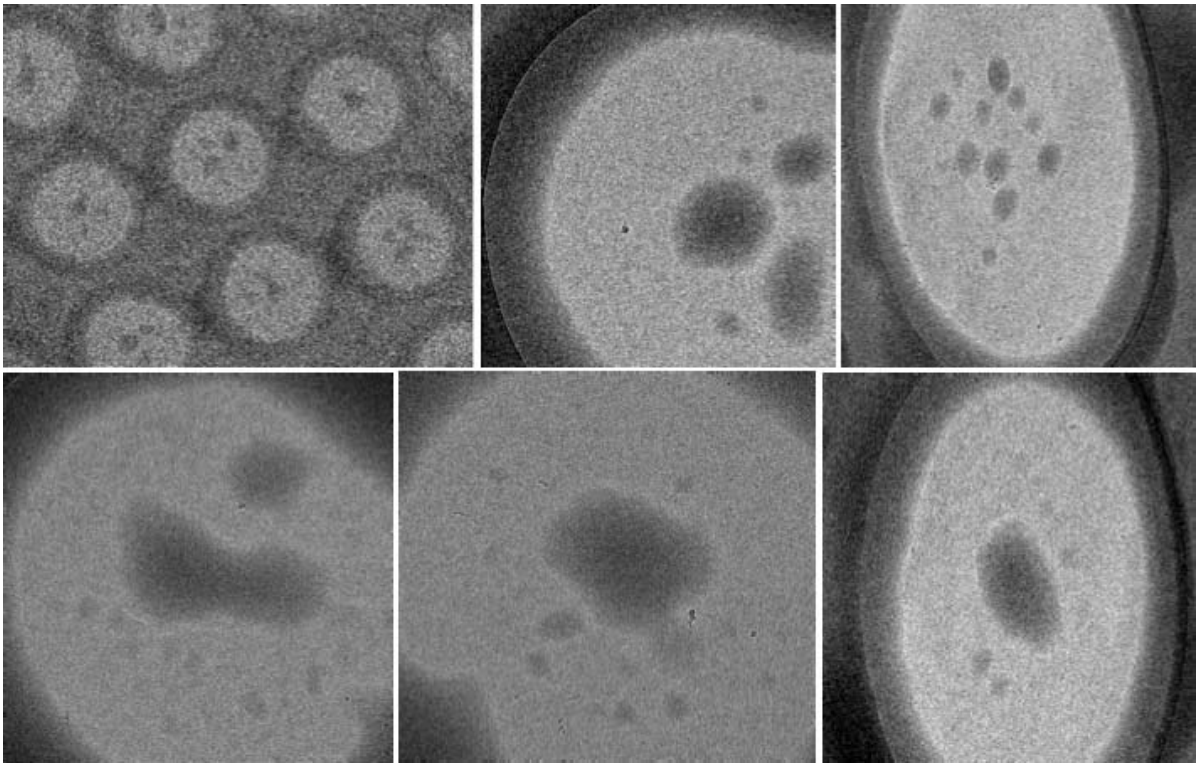

FIGURE S16. Cryo-EM single tomograms of wtAS sample incubated 3-5 days at 4 ˚C (latent acunas). A variety of shapes are apparent although the sizes are fairly regular. Similar forms are observed in liquid AFM (Fig. S9).

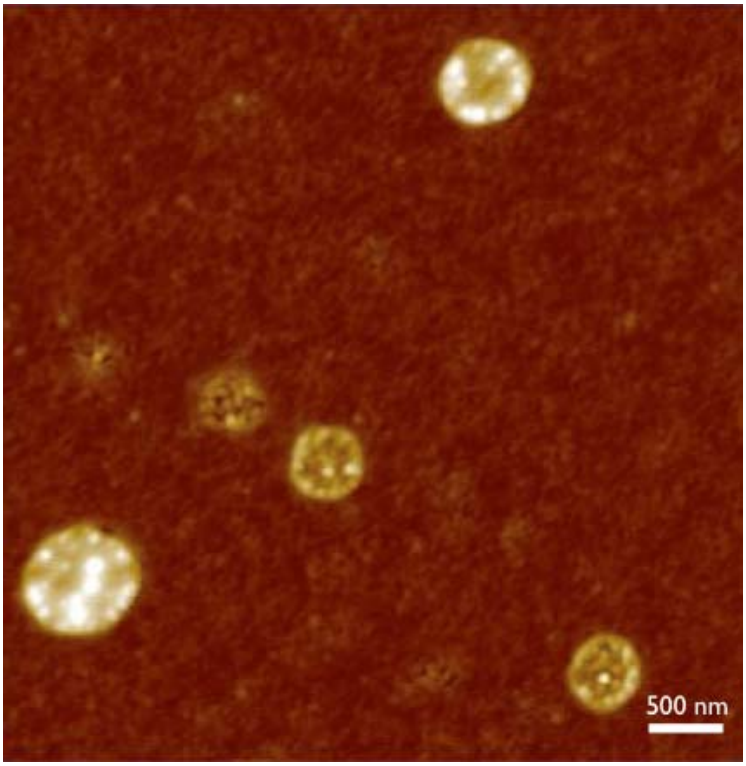

FIGURE S17. AFM image of latent acunas of wtAS incubated 3-5 days at 4 ˚C; preparation that was analyzed by Cryo-ET (Figs, 4 (man text), S15, 16).

Supporting References

1. Yushchenko, D. A., J. A. Fauerbach, S. Thirunavukkuarasu, E. A. Jares-Erijman, and T. M. Jovin. 2010. Fluorescent ratiometric MFC probe sensitive to early stages of α-synuclein Aggregation. *J. Am. Chem. Soc.* 132:7860-7861.
2. Thirunavukkuarasu, S., E. A. Jares-Erijman, and T. M. Jovin. 2008. Multiparametric fluorescence detection of early stages in the amyloid protein aggregation of pyrene-labeled α-synuclein. *J. Mol. Biol.* 378:1064-1073.
3. Starink, J. P. P., and T. M. Jovin. 1996. Background correction in scanning probe microscope recordings of macromolecules. *Surf. Sci.* 359:291-305.
4. Ermantraut, E., K. Wohlfart, and W. Tichelaar. 1998. Perforated support foils with predefined hole size, shape and arrangement. *Ultramicroscopy* 74:75-81.
5. Dubochet , J., M. Adrian, J. Chang, J. Homo, J. Lepault, A. McDowall, and P. Schultz. . 1988. Cryo-electron microscopy of vitrified specimens. *Q. Rev. Biophys.* 21:129-288.
6. Mastronarde, D. 2003 SerialEM A program for automated tilt series acquisition on Tecnai microcopes using prediction of specimen position. *Microsc. Microanal.* 9:1182-1183.